

Optimal Magnetic Bearing Control for High-Speed Momentum Wheels

Thomas Lange*

*Deutsche Forschungs- und Versuchsanstalt fuer Luft- und Raumfahrt e.V.
Oberpfaffenhofen, Federal Republic of Germany*

The magnetic bearing controller design described in this paper is based on the simplified equations describing linear gyroscopic systems. Their basic dynamic parameters are utilized in a numerical procedure to determine prescribed minimum gyroscopic damping coefficients. The system performance is optimized, with respect to the impact of sensor noise, by a gradient method using a minimum covariance criterion. The optimal performance requires an axis cross coupling, which at the same time provides damping of the satellite open-loop nutation oscillation.

Nomenclature

d	= normalized stator damping coefficient
$F_w(s); F(s)$	= wheel transfer function; complex notation
$G_c(s); G(s)$	= controller transfer function; complex notation
$H_w; H$	= wheel angular momentum; normalized value
I	= rotor transverse moment of inertia
I_s	= satellite transverse moment of inertia
I_w	= rotor spin axis moment of inertia
j	= imaginary unit
$k_w; k$	= rotary damping coefficient; normalized value
$L_c(s); L(s)$	= closed-loop transfer function; complex notation
M	= general matrix
p	= parameter solution vector
R	= sensor noise
S	= power spectral density
$s_i; \delta_i; \omega_i$	= i th complex eigenvalue; real, imaginary part
$T_{cx,z}; T_c$	= control torques; complex, normalized notation
$T_{x,z}; T$	= external torques on satellite; complex, normalized notation
T_s	= torque on wheel dynamics due to satellite motion
v	= general vector
$\alpha, \beta; \Gamma$	= relative angles of rotor tilt motion; complex notation
Δ	= relative damping
ϵ	= inter axis cross coupling
η	= ratio of rotor vs satellite transverse moment of inertia
λ	= lead ratio
$\rho_w; \rho$	= angular bearing stiffness; normalized value
σ	= covariance
$\tau_{zi}; \tau_{ni}$	= i th zero-, pole-time constant
$\phi, \psi; \Phi$	= roll, yaw satellite attitude angle; complex notation
θ	= pitch attitude angle
ω_0	= orbital angular rate
Ω	= wheel rotation speed

Subscripts

c	= controller
cr	= critical
i	= general index
j	= iteration index
nu	= nutation
pr	= precession
w	= wheel
x, z	= transverse axes

Superscripts

(\cdot)	= differentiation w.r.t. time
(T)	= matrix transposed
$(*)$	= conjugate complex

Introduction

MAGNETIC bearing technology, providing a contactless rotor suspension without friction losses and abrasion problems, permits in principle a very high rotation speed, i.e., stored angular momentum without loss of reliability. Therefore, flywheels equipped with these bearings are attractive for momentum stabilization of modern communication satellites with their multiple high-gain antenna systems requiring high-precision pointing control.

Momentum wheels of this type available today do not meet these ideal performance requirements. This is mainly due to low bearing stiffness, permitting compliant rotor motion. Through the strong bearing fields, this causes eddy current rotor losses with severe impact on satellite open-loop attitude stability. A similar effect has already been observed with the European Orbital Test Satellite (OTS 2) during stabilization with a compliant grease bearing wheel.¹ Experimental studies^{2,3} prove that this disadvantage can be overcome by an active bearing concept.

In Ref. 4, an explicit dynamical analysis is developed, which proves that only by an active wheel overall stability can be guaranteed during each phase of a satellite, i.e., also with the AOCS not being active. This paper presents a design method for a bearing controller that includes the respective overall stability condition.

Mathematical Model

The dynamics of a magnetically suspended rotor depend on the type of magnetic bearing being used. The bearing in general has a nonlinear characteristic, which is dependent on the specific hardware provided. In most cases, however, for

Table 1 Approximate eigenvalues

Eigenvalue	Eigenfrequency	Damping rate
Rotor precession	$\omega_p \approx -\rho/H$	$\delta_p \approx -\rho d/H^2 - (k + \epsilon\rho)/H$
Rotor nutation	$\omega_n \approx -H - \omega_p$	$\delta_n \approx -d - \delta_p$
Satellite nutation	$\omega_s \approx \alpha H$	$\delta_s \approx \alpha^2 H^3 (k/\rho + \epsilon)/\rho$

normal operation conditions, a linearization about a neutral point of operation is possible. With this assumption, the stabilization of the translational motion is fairly straightforward. The main problem is the spin-motor resonance due to mass unbalance. But in general, this can be accounted for by sufficient stability margin of the control loops. The rotor tilt motion, to be discussed in more detail, is largely defined by the gyroscopic eigenvalues and is almost independent of what type of controller is being used.

Structural dynamics can be excluded from this consideration, since they refer to the mechanical design, which is not discussed here. The respective frequencies either have to be kept out of the controller bandwidth, e.g., by an appropriate choice of rotor material, or the respective modal gains have to be small enough so as to guarantee minimum dynamic interference, which is a consideration for the stator and wheel housing design.

Hence, the basic dynamics of a spinning rotor are sufficient for modeling, where for a first approximation the bearing restraint torques can be described by the well-known spring-dashpot model used in general for mechanical systems.

Dynamics of Satellite: Satellite-Wheel System

The linearized equations of motion for satellite and wheel dynamics are explicitly derived in Ref. 4. With the axes defined as in Fig. 1, they are

Satellite:

$$I_{s,x}\ddot{\phi} + H_w\dot{\psi} + \omega_0 H_w\phi + I\ddot{\alpha} + H_w\dot{\beta} + \omega_0 H_w\alpha = T_x \quad (1a)$$

$$I_{s,z}\ddot{\psi} - H_w\dot{\phi} + \omega_0 H_w\psi + I\ddot{\beta} - H_w\dot{\alpha} + \omega_0 H_w\beta = T_z \quad (1b)$$

Wheel:

$$I\ddot{\phi} + H_w\dot{\psi} + \omega_0 H_w\phi + I\ddot{\alpha} + H_w\dot{\beta} + \omega_0 H_w\alpha + k_w(\dot{\alpha} + \Omega\beta) = T_{cx} \quad (2a)$$

$$I\ddot{\psi} - H_w\dot{\phi} + \omega_0 H_w\psi + I\ddot{\beta} - H_w\dot{\alpha} + \omega_0 H_w\beta + k_w(\dot{\beta} - \Omega\alpha) = T_{cz} \quad (2b)$$

The rotor losses, described by the coefficient k_w , produce damping torques proportional to the angular rates in the rotor-fixed coordinate frame. The predominant impact produced by the high rotor angular rate acts in the wheel coordinate frame as a cross-axis stiffness.

Neglecting second-order terms (i.e., excluding orbital rate coupling) and assuming overall symmetry (i.e., $I_{s,x} = I_{s,z} = I_s$), the equations now can be significantly simplified by normalization and complex notation,

$$\ddot{\Phi} - j\eta H\dot{\Phi} + \eta\ddot{\Gamma} - j\eta H\dot{\Gamma} = T \quad (3)$$

$$\ddot{\Phi} - jH\dot{\Phi} + \ddot{\Gamma} - jH\dot{\Gamma} - jk\Gamma = T_c \quad (4)$$

where

$$\begin{aligned} H &= H_w/I, & k &= k_w H/I_w, & \Phi &= \phi + j\psi, \\ \Gamma &= \alpha + j\beta, & T &= (T_x + jT_z)/I_s, & T_c &= (T_{cx} + jT_{cz})/I \end{aligned}$$

For an approximate analysis, the control torque T_c can be described by an angular stiffness and damping parameter, ρ

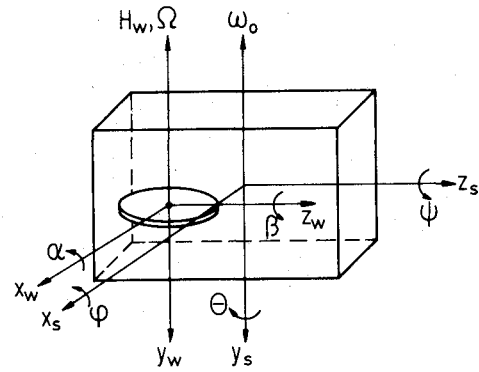


Fig. 1 Satellite-wheel coordinate frame.

and d , respectively. An active cross coupling is provided by the coupling factor ϵ ,

$$T_c = -[d\dot{\Gamma} + \rho(I - j\epsilon)\Gamma] \quad (5)$$

The result of the approximate eigenvalue analysis according to Ref. 4, is listed in Table 1. Two parameters, H and ρ , essentially determine the *gyroscopic* eigenfrequencies. In the following, they are referred to as *basic* parameters.

The damping characteristic is determined by the three parameters d , k , and ϵ . The critical parameter, generating satellite nutation instability, is the coefficient k , which has been explicitly discussed in Ref. 4. A necessary stability condition is

$$k + \epsilon\rho < 0 \Rightarrow \epsilon < -k/\rho \quad (6)$$

There is, however, an inverse effect of the active cross-coupling coefficient ϵ on rotor precession damping, indicating that this parameter is essential for the controller design.

Transfer Function of Wheel Dynamics

The bearing controller design is performed in the frequency domain. The schematic representation in Fig. 2 shows the functional implementation of the controllers with the cross coupling at their outputs. According to the complex notation of Eq. (4), this control scheme can also be represented by one single loop containing transfer function blocks with complex coefficients. Their real part represents the transfer function from roll (yaw) input to roll (yaw) output, whereas the imaginary part describes the cross-axis dynamics.

The satellite dynamics can be represented by an additional torque input T_s , while neglecting the weak mutual dynamic coupling. This also holds for the structural resonances of flexible appendages, if the modal gain factors involved are small. Hence, the wheel dynamics are essentially determined by the closed-loop transfer function according to Fig. 3, yielding the characteristic equation

$$I + F(s)G(s) = 0 \quad (7)$$

Control Method

The controller design is strongly dependent on the mission requirements and hardware constraints. They largely define the operating conditions and the optimization criterion as well.

Requirements and Constraints

The most important requirements under normal operational conditions are a high stored angular momentum to increase the pointing accuracy and a large bearing stiffness to avoid a wheel touchdown as a result of external torques. A control concept delivering this performance can be realized only by

providing large gain and bandwidth, since the gyroscopic eigenfrequencies diverge strongly with increasing wheel speed. A minimum stability margin has to be guaranteed during all operational phases, including the spin-up period.

A common problem associated with high-gain broadband control loops is the sensor noise sensitivity, which may lead to amplifier saturation and power losses at the output. The kind of noise to be expected is introduced via coupling into the magnetic pickoff systems commonly used to control the gaps. It is generated essentially by the geometrical imperfections of the bearing itself and the stray field of the spin motor. With this kind of broadband noise, it is reasonable to reduce the controller bandwidth by introducing minimum damping constraints to be exceeded not unnecessarily.

Sufficient precessional damping is essentially required to reduce the dynamic response time after an external disturbance, while nutation, being a high-frequency motion, requires just a sufficient stability margin. As relative nutation damping usually decreases with rotor speed, the constraint to be realized is a minimum damping ratio at maximum specified rotor speed. Precessional damping requirements, however, can be reasonably guaranteed by prescribing a fixed damping ratio at nominal rotor speed and a tolerance margin during the spin-up phase.

The additional eigenvalues generated by the dynamic feedback are not critical, as they are strongly damped as compared to the dominant gyroscopic modes.

Basic Structure of the Control Network

The controller is assumed to consist of two cross-coupled cascaded lead networks, which can be easily realized by ordinary active filters. Formally, the transfer function given in Fig. 4 includes also the sensor and actuator performance to be approximated by low-pass filters. This characteristic, including that of the controller, can be approximated by a single overall roll-off frequency given by the time constant τ_{n4} .

Practical design experience has shown that at least three single lead networks are required in a cascade to yield reasonable ratios τ_{zi}/τ_{ni} . However, additional networks may be useful, depending on the actual wheel parameters. The same is applicable to the roll-off characteristic, which may require more than one low-pass filter, as shown here.

The sensor noise at the input is assumed to be white Gaussian noise. This does not fully comply with the kind of disturbances according to the requirements and constraints analysis summarized above. However, as the real noise characteristic is not exactly known, this approach is used to deal with the expected broadband characteristic of the disturbances.

Parameter Optimization

The optimization is performed by an iterative searching routine in a hierarchical organization. The basic idea of how to minimize the noise at the controller output is gain reduction, utilizing the physical laws of gyroscopic motion embodied in the simplified model presented above. To this end, the different lead networks are associated with individual gyroscopic modes to be controlled. Basically, these are precession and nutation, which require two stabilizing networks for normal operational conditions. However, during spin-up, these modes vary significantly, which is accounted for by the third network. It is associated with a gyroscopic mode at a critical wheel speed to be determined during the optimization. The critical mode is the rotor precession, which can be understood from the approximate formulas given in Table 1, which show that precessional damping decreases with a coupling factor ϵ according to Eq. (6).

Direct Solution Approach

For the inner loop of this optimization routine, a direct solution of the characteristic equation with respect to the rele-

vant parameters is provided in Ref. 5. With a configuration according to Fig. 4, the basic relation given by Eq. (7) becomes

$$\rho(1-j\epsilon) \prod_{i=1}^3 (1+\tau_{zi}s) + (s^2-jHs-jk) \prod_{i=1}^4 (1+\tau_{ni}s) = 0 \quad (8)$$

First-order approximations to the dominant gyroscopic eigenvalues are found by using the expressions listed in Table 1,

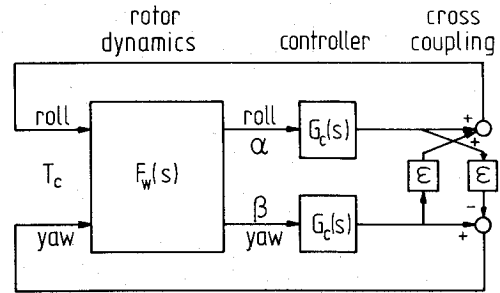


Fig. 2 Schematic of bearing control loop.

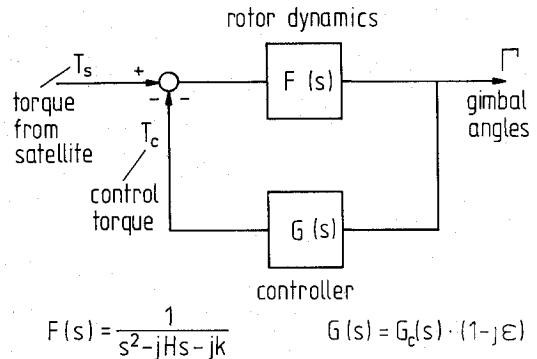


Fig. 3 Block diagram of closed-loop wheel dynamics.

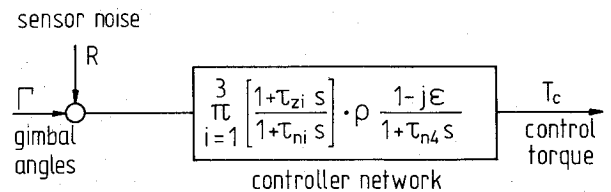


Fig. 4 Controller structure.

Table 2 Controller design data

Parameter	Value
Wheel data	
Angular momentum (nom.)	$H_w = 100 \text{ N} \cdot \text{ms}$
Rotation speed (nom.)	$\Omega = 1689 \text{ rad/s}$
Rotor transverse moment of inertia	$I = 33.7 \times 10^{-3} \text{ kgm}^2$
Spin axis moment of inertia	$I_w = 59.2 \times 10^{-3} \text{ kgm}^2$
Radial bearing stiffness	$\rho_w = 965 \text{ Nm/rad}$
Rotary damping parameter	$k_w = 0.01 \text{ N} \cdot \text{ms/rad}$
Design goal	
Relative nutational damping (max./speed)	$\Delta_{nu} = 5\%$
Relative precessional damping (nom. speed)	$\Delta_{pr} = 30\%$
Minimum relative damping (spin-up phase)	$\Delta_{\min} = 20\%$

supplemented by the damping rates δ to be achieved,

$$\text{Nutation:} \quad s_{nu} = \delta_{nu} + jH \quad (9a)$$

$$\text{Precession:} \quad s_{pr} = \delta_{pr} + j\rho/H \quad (9b)$$

Inserting these into Eq. (8) yields four independent equations permitting the computation of four parameters, i.e., two frequency sensitive and two damping sensitive parameters. The frequency sensitive ones are the basic parameters as defined previously, i.e., the rotor angular momentum H and the angular bearing stiffness ρ . They are predetermined by the design requirements. The computed values H_j and ρ_j , at the j th iteration step are utilized for eigenfrequency updating at the $(j+1)$ th step:

$$\omega_{nu,j+1} = H/H_j \omega_{nu,j} \quad (10a)$$

$$\omega_{pr,j+1} = H/H_j \omega_{pr,j} \quad (10b)$$

until the computed parameters cover vs the basic parameters H and ρ . Thus, an exact solution for two damping sensitive (i.e., the control parameters) can be found, while the rest is left for the superimposed loops of the optimization procedure.

With the intuitive assumption that the two networks to be determined here are most effective in terms of the minimum controller gain required, with their center frequency tuned to the eigenfrequencies with which they are associated, the number of parameters to be determined can be reduced. The center frequency, ω_i of the i th network is defined by the relation

$$G_i(s) = \frac{I + \tau_{zi}s}{I + \tau_{ni}s} = \frac{I + (\lambda_i/\omega_i)s}{I + (I/\lambda_i\omega_i)s} \quad (11)$$

where

$$\lambda_i = \sqrt{\tau_{zi}/\tau_{ni}}, \quad \omega_i = \sqrt{I/\tau_{zi}\tau_{ni}}$$

With the tuning condition, i.e., $\omega_i \approx \omega_{nu}$ (or ω_{pr} respectively), the damping parameters to be computed here are λ_i , referred to as lead ratios.

The computation in general requires the solution of a nonlinear equation. This is extracted from a linear relation

$$M_j p_j = v_j \quad (12)$$

derived from Eq. (8) for each iteration step j , where p_j is a solution vector exclusively containing the parameters to be computed during this step. The solution of Eq. (12) is not unique and thus requires a decision on which one is to be selected to solve the control problem.

Precessional Damping

The precession solution vector $p_{pr,j}$ has three elements containing the angular bearing stiffness coefficient ρ_j and the lead ratio λ_{pr} of the network associated with precession damping,

$$p_{pr,j}^T = [\rho_j, \rho_j \lambda_{pr}, I/\lambda_{pr}] \quad (13)$$

The element $p_3 = 1/\lambda_{pr}$ defining the eigenvalue damping requires the solution of a *second-order* equation, where in principle there may be no useful solution at all if the result is complex. Otherwise, two solutions exist. In this case, the problem is not severe, since with the small damping ratios required a real solution will always be obtained. The uniqueness is usually guaranteed by the obvious stability requirement that λ_{pr} has to be positive.

Nutational Damping

With the basic frequency parameter H_j , the solution vector $p_{nu,j}$, which determines nutational damping, has four elements,

$$p_{nu,j}^T = [H_j, H_j/\lambda_{nu}, I/\lambda_{nu}, \lambda_{nu}] \quad (14)$$

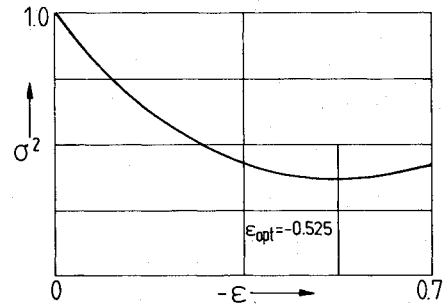


Fig. 5 Relative covariance with respect to the cross-coupling factor ϵ .

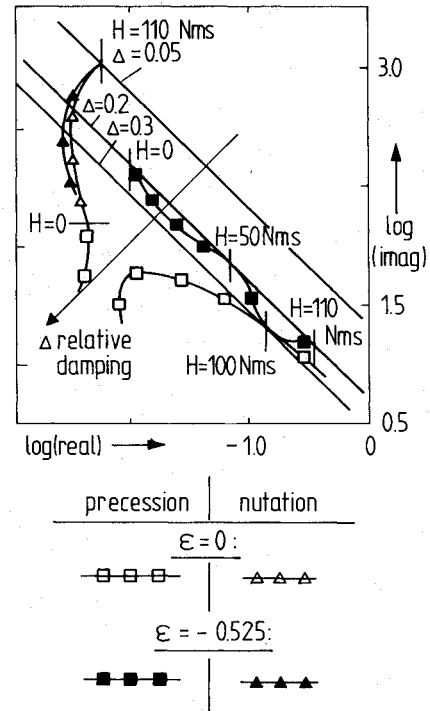


Fig. 6 Root locus of gyroscopic eigenvalues.

A *third-order* equation can be derived for the damping sensitive parameter, $p_4 = \lambda_{nu}$. Again, there is, in principle, no unique solution, but at least one is real and can be assumed to be practically stable for the same reasons as before. In case of multiple real solutions, the maximum is chosen in order to keep the dynamic gain as small as possible and supposing that this one at least will be stable, if the other two should not be.

Gradient Method Optimization

The criterion for optimum performance is the average power at the controller output due to input sensor noise. It is minimized by applying a gradient method covering the parameters not yet constrained by the tuning process. These coefficients are primarily the cross-coupling factor ϵ and the time constant τ_{n4} defining the roll-off frequency. To demonstrate the dependence upon cross coupling, the optimization is performed stepwise with ϵ being parametrically changed.

In addition, the lead network center frequencies are included. This is especially required for the nutation network as, due to the closely spaced roll-off frequency, the tuning hypothesis for this mode does not fully comply with the gradient optimization results. However, the tuning method is still used for generating the appropriate initial conditions.

Finally, the critical rotor speed Ω_{cr} is determined in this loop. It is defined by the minimum precession damping during

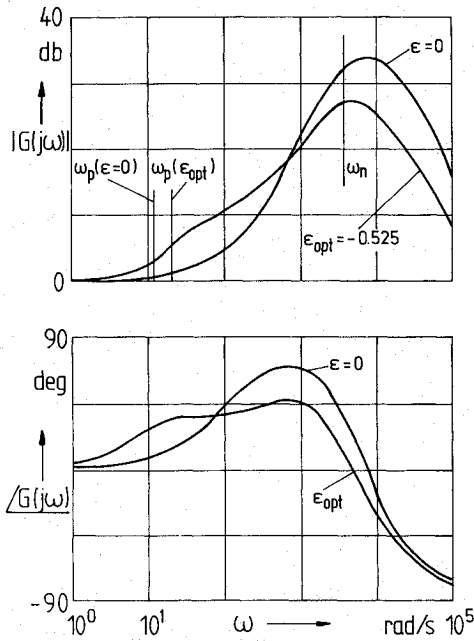


Fig. 7 Bode plot of controller transfer function.

the spin-up period and is evaluated by a stepwise eigenvalue analysis. The respective wheel parameter H_{cr} is used to find a direct solution for the third lead network within the inner loop.

Noise Covariance

The noise transfer function of the wheel is defined according to Figs. 3 and 4 by

$$L(s) = \frac{\Gamma(s)}{R(s)} = \frac{G(s)}{1 + F(s)G(s)} \quad (15)$$

The total power via the direct and cross-axis transfer functions due to a noise input requires the conjugate complex transfer functions to be multiplied according to the well-known relation,

$$S(j\omega) = L(j\omega)L(-j\omega)S_0 \quad (16)$$

where S_0 denotes the constant white noise input power spectral density and $S(j\omega)$ the respective parameter at the controller output.

The average power, dissipated at the outputs, can be computed via the inverse Fourier transformation, yielding the autocorrelation function and setting the time interval equal to zero. The inverse transformation is performed by computation of the residuals after determination of the closed-loop eigenvalues s_v of the transfer function $L(j\omega)$. As no multiple poles are present, the residuals compute simply as

$$\sigma^2 = \sum_v \lim_{s \rightarrow s_v} S(s)(s - s_v) \quad (17)$$

where σ denotes the output noise covariance.

Numerical Results

The design procedure outlined so far has been numerically verified using the parameters of the active bearing momentum wheel MDR100-1 by TELDIX (Germany) and SEP (France), which is considered to be typical for possible future applications. Some values have been determined through dynamic testing, e.g., the angular stiffness and rotary damping parameter, ρ_w and k_w , respectively.³

Covariance

In Fig. 5, the noise covariance is given in relative values with respect to zero cross coupling, since the absolute mean power of the assumed input white noise is infinite. This method is realistic as long as the bandwidth of the actual noise exceeds that of the controller. As a first approximation it can be assumed, according to Eq. (16), that the mean power dissipation at the output is proportional to the integral over frequency of the controller dynamic gain squared. Considering the cross-coupling influence on gyroscopic mode damping as derived from the dynamic model, the nutation damping increases with increasing $|\epsilon|$ and thus requires less controller phase lead and hence dynamic gain. However, the precessional motion being inversely influenced, requires additional phase lead from the controller, thus enhancing the dynamic gain. Due to these counteracting effects, an optimum occurs at $\epsilon = -0.525$.

The satellite nutation at this design point is asymptotically stable, being far from the stability boundary. Assuming, for example, a satellite with a transverse moment of inertia of 3000 kgm², the relative satellite nutation damping is yet $\Delta_s = 1.7 \times 10^{-3}$.

Root Locus

The location of the precession and nutation poles with respect to the rotor speed shows the stability margin obtained by this kind of control. In Fig. 6, these values are plotted in a double logarithmic scale for $\epsilon = 0$ and for the optimal value $\epsilon = -0.525$. Note, that for zero cross coupling, i.e., $\epsilon = 0$, the precessional damping values for low angular momentum are outside the prescribed band of relative damping. In contrast to that, the optimal case is characterized by a minimum damping of $\Delta_{pr} = 0.2$ at $H_w = 50$ N·m/s and $\Delta_{pr} \leq 0.3$ anywhere else. It is not possible to maintain this band of relative damping for $\epsilon = 0$, as the results obtained numerically demand excessive lead ratios for the nutation stabilizing network.

Controller

An optimal ($\epsilon = -0.525$) and a zero cross-coupling transfer function are compared to each other in Fig. 7. The optimum is characterized by a smaller amplitude peak and also by a lower maximum phase lead value, but by a large bandwidth similar to the nonoptimal case. The bandwidth is primarily determined by the nutation frequency, i.e., $\omega_{nu} = 2.9 \times 10^3$ rad/s for nominal wheel speed. However, the Bode plot shows a frequency range in excess of that which may impose problems with the higher-order dynamics of the control system. This can be accounted for by respective additional transfer functions, augmenting the controller transfer function according to Fig. 4, if these influences cannot be modeled by an effective roll-off frequency according to what has been assumed so far. Experimental investigations³ indicate that this is possible, since the measured transfer functions in the high-frequency range show a significant peaking only at the nutation frequency. Hence, the assumption of the gyroscopic frequencies being dominant as compared to higher-order dynamics is valid.

In addition to that, a further bandwidth reduction can be achieved by controller resident filters to be included in the optimization. But it should be noted, after all, that the bandwidth problem is not specific to the design method presented here, but is associated with the problem of high nutation frequency control in general. Hence, this parameter is the most critical one for the bearing controller design determining to a large extent the feasibility of high-speed momentum wheel stabilization.

Conclusions

A design procedure for an optimal magnetic bearing controller has been presented using the mechanical model of a spinning rotor. This method reduces the design complexity and improves the physical interpretation of the performance

significantly. The proposed design provides low gain values and thus an optimal input noise response characteristic. An internal axes cross coupling included in the optimization provides at the same time open-loop satellite nutation damping and hence an overall stability during all mission phases.

References

¹Lacombe, J.L., Delaunay, M., Pelta, G., Legars, A., "Study of OTS 2 Inflight Behaviour. Nutation Interaction with Momentum Wheel," MATRA Espace, European Space Agency, Contractors Report 1328, 1979.

²Rouyer, C., Heimbold, G., and Lange, Th., "Analysis and Experimental Verification of the Nutation of a Satellite Equipped with Magnetic Bearing Momentum Wheels," *Spacecraft Pointing and Position Control*, AGARDograph 260, 1981, pp. 2-1—2-19.

³Heimbold, G. and Lange, Th., "Final Report: Dynamic Investigation on the Active Magnetic Bearing Momentum Wheel MDR100-1, manufactured by TELDIX (FRG) and SEP (France), DFVLR, Oberpfaffenhofen, FRG, 1981.

⁴Heimbold, G., "Magnetic Bearing Momentum Wheels—Impact of Bearing Design on Nutational Stability of Satellites," *Journal of Guidance, Control, and Dynamics*, Vol. 7, May-June 1984, pp. 279-285.

⁵Siljak, D.D., "Nonlinear Systems," *The Parameter Analysis and Design*, John Wiley & Sons, New York, 1969, Chap. 1.

From the AIAA Progress in Astronautics and Aeronautics Series

SPACE SYSTEMS AND THEIR INTERACTIONS WITH EARTH'S SPACE ENVIRONMENT—v. 71

Edited by Henry B. Garrett and Charles P. Pike, Air Force Geophysics Laboratory

This volume presents a wide-ranging scientific examination of the many aspects of the interaction between space systems and the space environment, a subject of growing importance in view of the ever more complicated missions to be performed in space and in view of the ever growing intricacy of spacecraft systems. Among the many fascinating topics are such matters as: the changes in the upper atmosphere, in the ionosphere, in the plasmasphere, and in the magnetosphere, due to vapor or gas releases from large space vehicles; electrical charging of the spacecraft by action of solar radiation and by interaction with the ionosphere, and the subsequent effects of such accumulation; the effects of microwave beams on the ionosphere, including not only radiative heating but also electric breakdown of the surrounding gas; the creation of ionosphere "holes" and wakes by rapidly moving spacecraft; the occurrence of arcs and the effects of such arcing in orbital spacecraft; the effects on space systems of the radiation environment, etc. Included are discussions of the details of the space environment itself, e.g., the characteristics of the upper atmosphere and of the outer atmosphere at great distances from the Earth; and the diverse physical radiations prevalent in outer space, especially in Earth's magnetosphere. A subject as diverse as this necessarily is an interdisciplinary one. It is therefore expected that this volume, based mainly on invited papers, will prove of value.

Published in 1980, 737 pp., 6×9, illus., \$35.00 Mem., \$65.00 List

TO ORDER WRITE: Publications Order Dept., AIAA, 1633 Broadway, New York, N.Y. 10019